MAPPING ALTIMETRY IN THE FORTHCOMING SWOT ERA BY BACK-AND-FORTH NUDGING A ONE-LAYER QUASI-GEOSTROPHIC MODEL.

Florian Le Guillou[1], Sammy Metref[1], Emmanuel Cosme[1], Clément Ubelmann[2], Maxime Ballarotta[3], Julien Le Sommer[1], and Jacques Verron[1,2]

[1]*Université Grenoble Alpes, CNRS, IRD, Grenoble INP, IGE; Grenoble, France*
[2]*Ocean Next, Grenoble, France.*
[3]*Collecte Localisation Satellites, Ramonville St-Agne, France*

Supplemental Material

1 Introduction

In the main document, we have shown the relevance of a data assimilation algorithm, the BFN-QG, to map SSH from nadir and SWOT data in a highly dynamical region (namely the GULFSTREAM region). The BFN-QG has been tested in the framework of OSSE with current (nadir) and future (SWOT-like) realistic altimetric observations. The SSH maps, provided by different observational scenario, have been systematically compared to conventional DUACS products. The comparison has been made during a time period extending over two months, from April 1, 2013, to July 1, 2013.

We propose in this document to assess the robustness of the BFN-QG algorithm to geographical region and seasonal changes. In section 2, we present the results of the mapping performances obtained in winter (February-March) and summer (August-September). Only the scenario where Nadir and SWOT data are assimilated all together is presented. In section 3, we focus on another region, namely the OSMOSIS region. All experiences performed for the GULFSTREAM region remain the same, with a few adjustments to some of the parameters of the algorithm.

2 Robustness to seasonal change

Recent model-based studies suggest that the ocean upper layer (sub)mesoscale dynamics has a strong seasonality (Ajayi et al., 2020; Uchida et al., 2017). In particular, winter is marked by the apparition of small vortices (<50km) associated with mixed layer instabilities. In Ajayi et al. (2020), the authors have shown that the mean eddy scale in summer is twice as large as in winter in the NATL60 simulation.

In the main document, we chose to compare the BFN with DUACS over one intermediate season, in spring, in order to be as general as possible. However, it is scientifically interesting to test our mapping technique over other time periods, to check the consistency of the method over different dynamical regimes.

Two other experiments have been carried out in the GULFSTREAM region: one in winter (from January 1, 2013, to April 1, 2013), the other in summer (from July 1, 2013, to October 1, 2013). As in the main article, the first month of each period is considered as a spin-up period and is not considered in the diagnostics. We focus here only on the constellation of SWOT and Nadir satellites. All the parameters relative to the BFN-QG algorithm are identical to the ones used in the main document.

Figures 1 and 2 illustrate examples of snapshots of the nature run (NR; i.e. the "true" state of the ocean) and the reconstructions from DUACS and BFN-QG for the two seasons. We can clearly see on the vorticity snapshots (bottom left panels) the increase of the number of submesoscale vortices in winter compared to summer.

The performances of the reconstructions for the two seasons are reported on Figures 4 and 3. The diagnostics show that whatever the season (winter, spring, summer), the BFN-QG outperforms the DUACS method, whether in terms of RMSE or PSD. One particularly interesting feature is that the spatial resolution of the maps derived by the BFN-QG algorithm is the same in winter and summer, what shows a strong robustness of the method according to the dynamical regime.

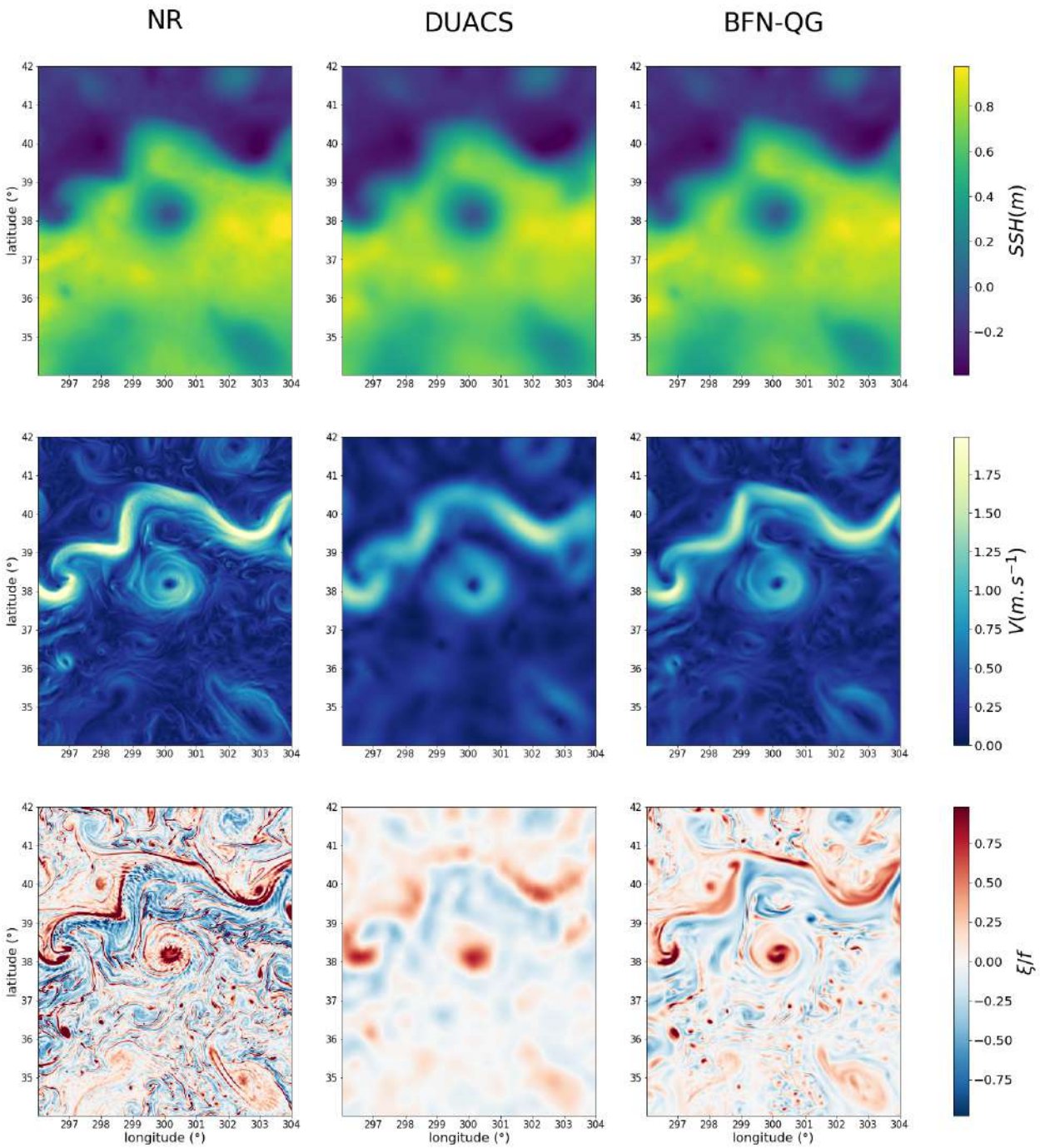

Figure 1: Snapshots of SSH (top), absolute geostrophic velocity (middle line) and normalized geostrophic relative vorticity (bottom) for the NR (left), DUACS (middle column) and BFN-QG (right) on February 25, 2013 in the GULFSTREAM region. DUACS and BFN-QG are processing both nadir and SWOT data. Velocity and relative vorticity maps are computed on the native grids, i.e. before the interpolation to the (1/60° x 1/60°) grid of the NR.

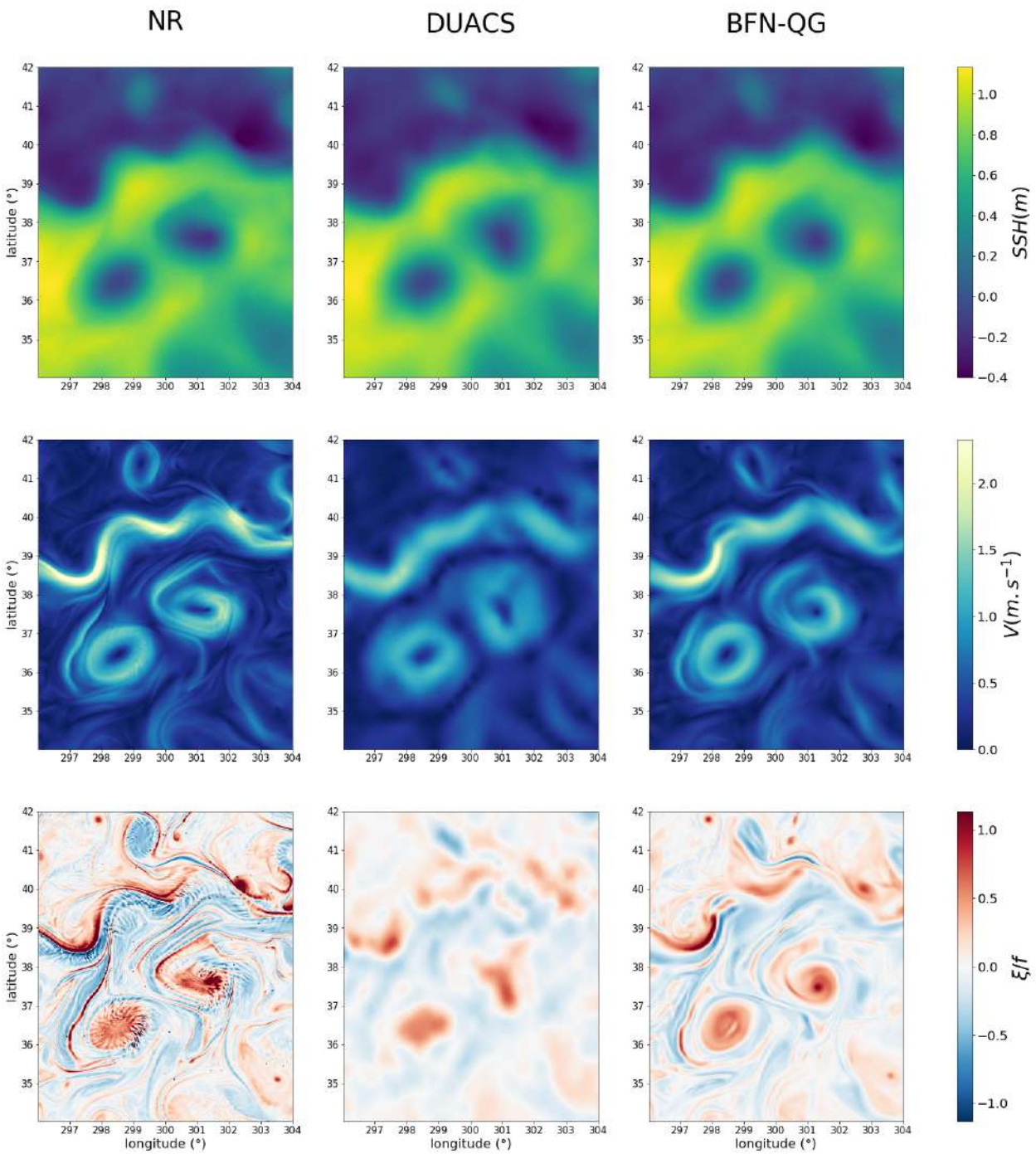

Figure 2: Same as Figure 1 but on August 19, 2013

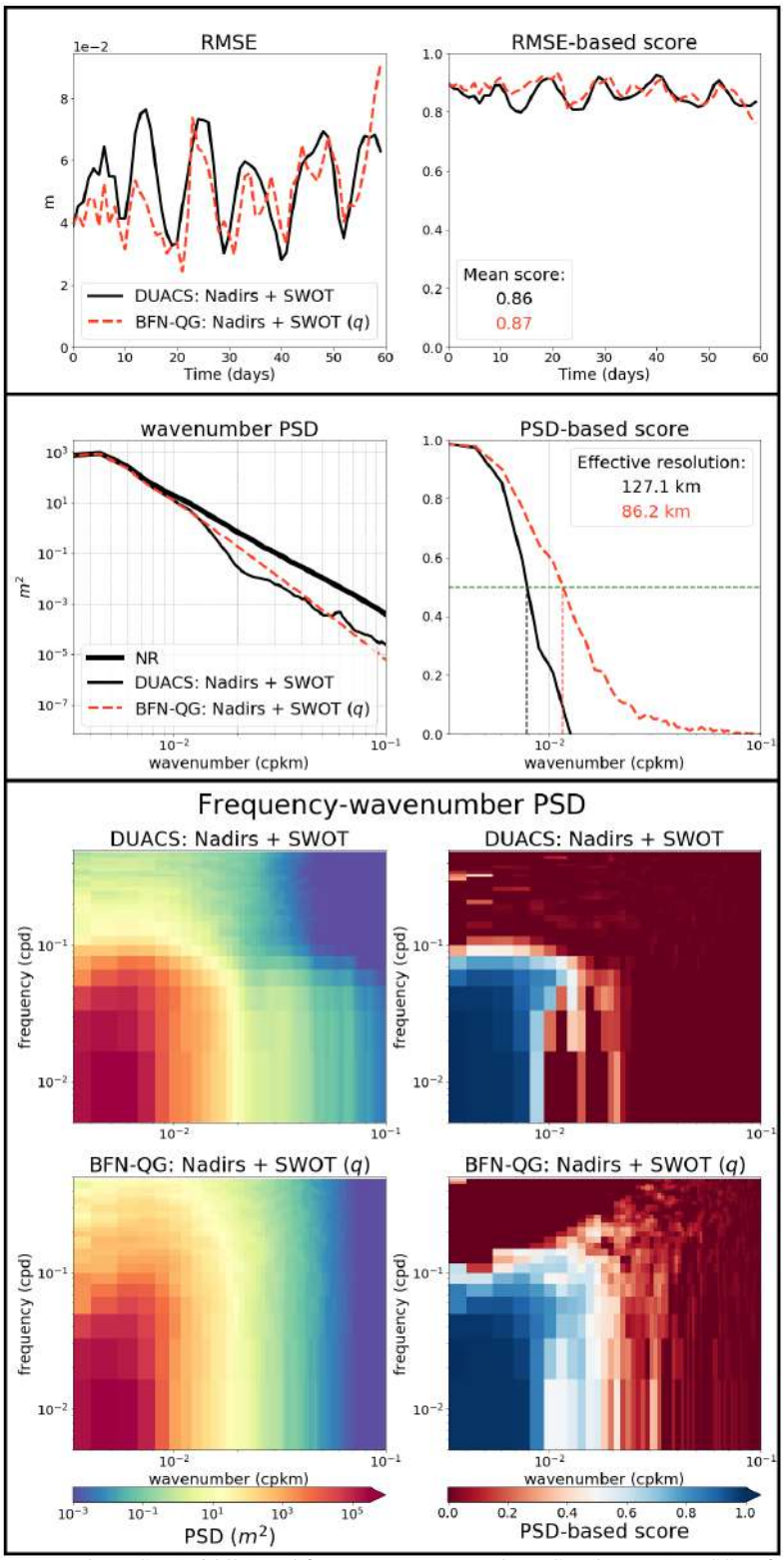

Figure 3: RMSE (top), wavenumber PSD (middle) and frequency-wavenumber PSD (bottom) on SSH, for DUACS and BFN-QG with SWOT and nadir altimeters altogether in winter (February and March 2013).

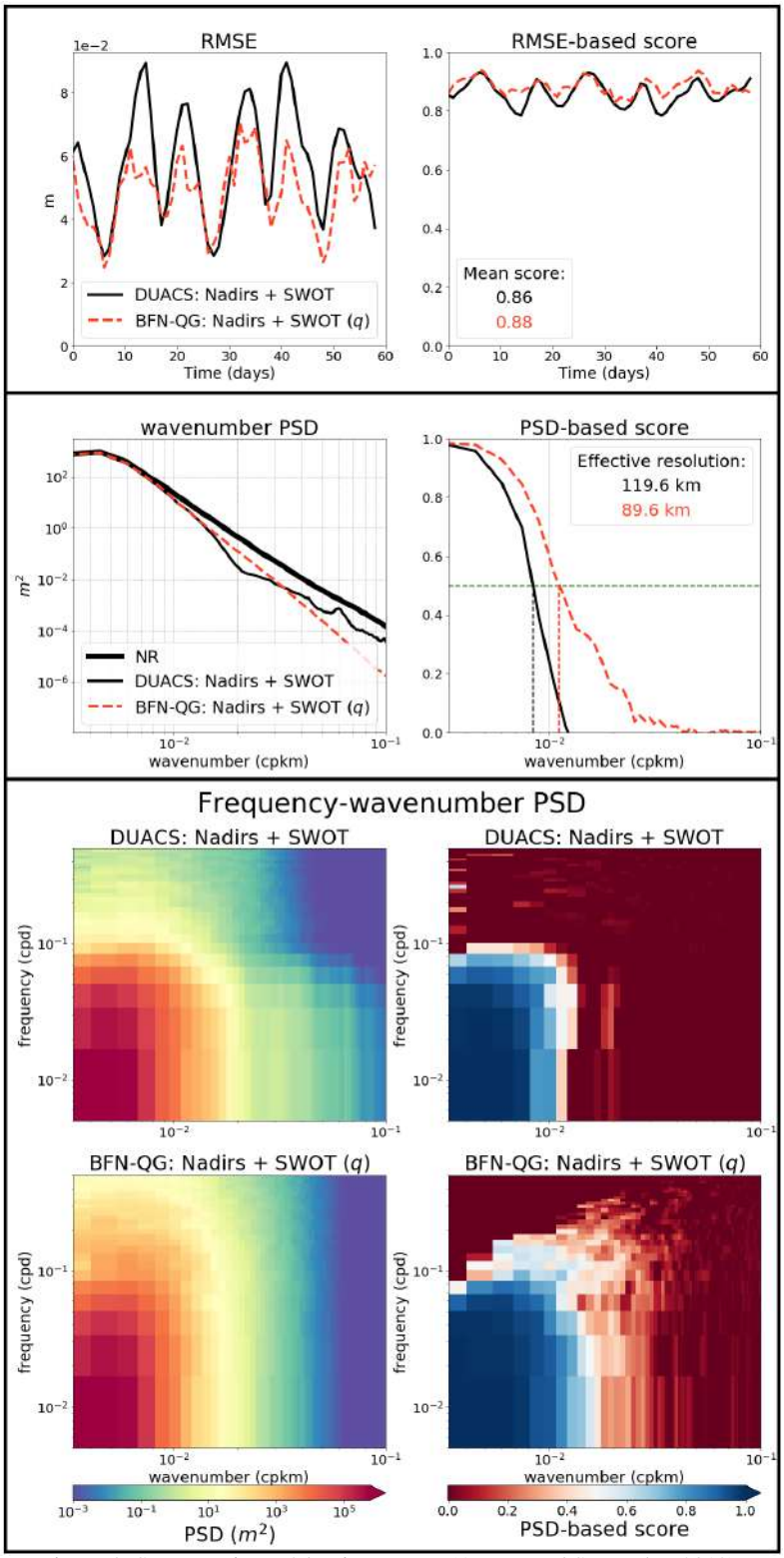

Figure 4: Same as Figure 3 but in summer (August and September 2013).

3 Robustness to geographical region change

3.1 The OSMOSIS region

Figure 5: SSH snapshots (in m) of the two studied regions from the NR on May 26, 2013. On the left, the GULFSTREAM region, with SSH ranging from $-0.4m$ to $1m$. On the right, the OSMOSIS region, with SSH ranging from $-0.4m$ to $0.2m$.

The OSMOSIS region is a ten by ten degrees box located on the Porcupine Abyssal plain, as represented in figure 5. The choice of this regions is made essentially for two reasons. First, the OSMOSIS region is less energetic than the GULFSTREAM region, with more discernible small scale processes. Figure 6 illustrates this dynamical difference by showing the frequency-wavenumber power spectral density, which provides a description of the resolved scales both in space and time. In this figure, we clearly see that the GULFSTREAM region exhibits physical processes 100 times more energetic at scales $< 10^{-2}$cpkm (> 100km) and that this high energy is associated with physical processes presenting a higher temporal variability compared to the OSMOSIS region. Besides, the spatial gradient of energy around 100km is less pronounced in the OSMOSIS region, revealing finer structures at scales < 100km. Second, the OSMOSIS region differs from the GULFSTREAM region by the difference in temporal samplings of SWOT due to their different latitude locations, with a regular sampling in the OSMOSIS region (one SWOT observation every day) versus an irregular sampling in the GULFSTREAM region (time periods of several days without observations).

3.2 Configuration of the BFN-QG

In this section, we detail the tunable parameters of the BFN-QG algorithm that differ in the two regions: the Rossby radius of deformation L_R, the nominal nudging coefficient K_0 and the nudging temporal window τ.

Following Chelton et al. (1998), L_R is set equal to 20km in the OSMOSIS region (versus 30km in the GULFSTREAM region). This corroborates the fact that the OSMOSIS displays finer mesoscale structures than the GULFSTREAM region.

The nudging parameters (K_0 and τ) are listed in table 1. As a reminder, we show also the parameters set for the GULFSTREAM region. The OSMOSIS region being less energetic than the GULFSTREAM region, the correlation time scale of the flow is longer. That is why τ is higher in OSMOSIS than in GULFSTREAM for nadir data. Yet, for SWOT data, τ was set higher in GULFSTREAM to compensate its poor temporal sampling in this region.

3.3 Results

Figures 7, 8, 9, and 10 are in the same format than in the main document, but for the OSMOSIS region. The results are qualitatively similar to the GULFSTREAM region, so that the analysis conducted in Section 4 in the main document holds. The main two differences are:

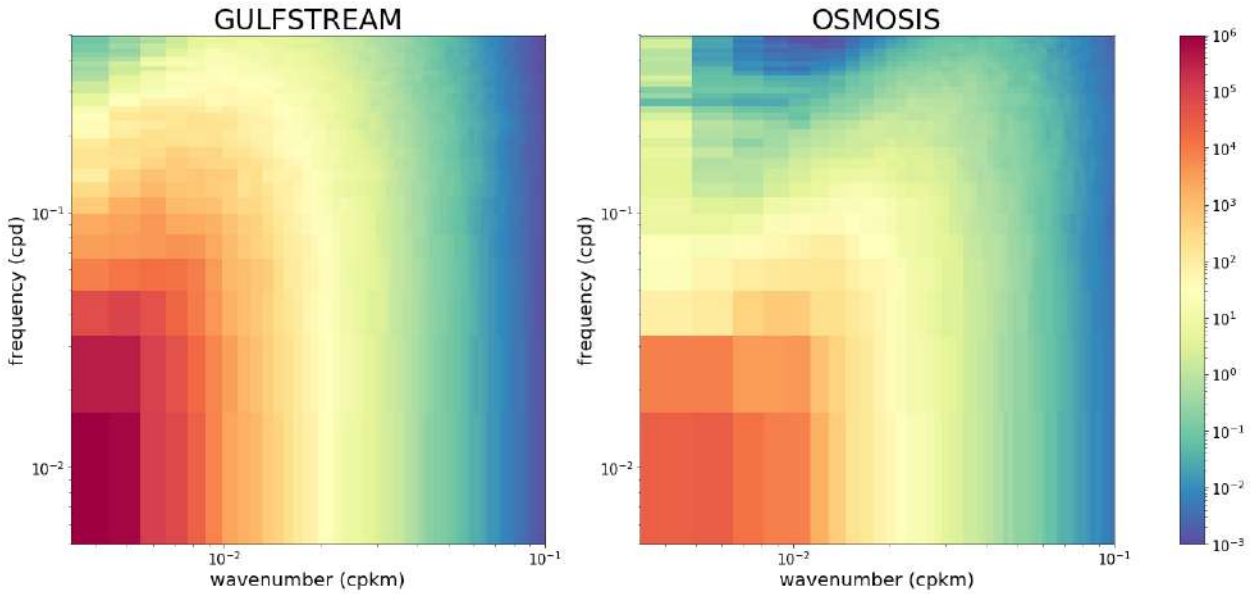

Figure 6: SSH Frequency-wavenumber spectra (in m^2) of the two studied regions from May 1, 2013 to July 1, 2013.

Satellites	$K_0 dt$		τ (days)	
	GS	OSMO	GS	OSMO
Nadirs (SSH)	0.9	0.1	1	2
SWOT (SSH)	0.9	0.7	2	1
SWOT (ξ)	0.05	0.05	1	0.5

Table 1: Nudging parameters used in the experiments according to the kind of altimetric sensor (nadir or SWOT), the studied region (GS for GULFSTREAM, OSMO for OSMOSIS) and the variable nudged (SSH/ξ)

- The effective resolution is generally better in the OSMOSIS region than in the GULFSTREAM region. This is very likely due to a less intense dynamics in the former, and to more frequent revisits of the satellite in the OSMOSIS region, located at latitudes higher than the GULFSTREAM region;
- The RMSE time series for the experiment including SWOT do not exhibit regular oscillations as in the GULFSTREAM region. In the latter, the oscillations are due to a five-day period without any SWOT pass. This is not the case in the OSMOSIS region, because of the region location again.

Although the experiments in the OSMOSIS region are very different in terms of mapping challenges to the ones in the GULFSTREAM region, the improvement brought by the dynamical constraint, i.e. the BFN-QG, in the mapping reconstruction is confirmed in the OSMOSIS region.

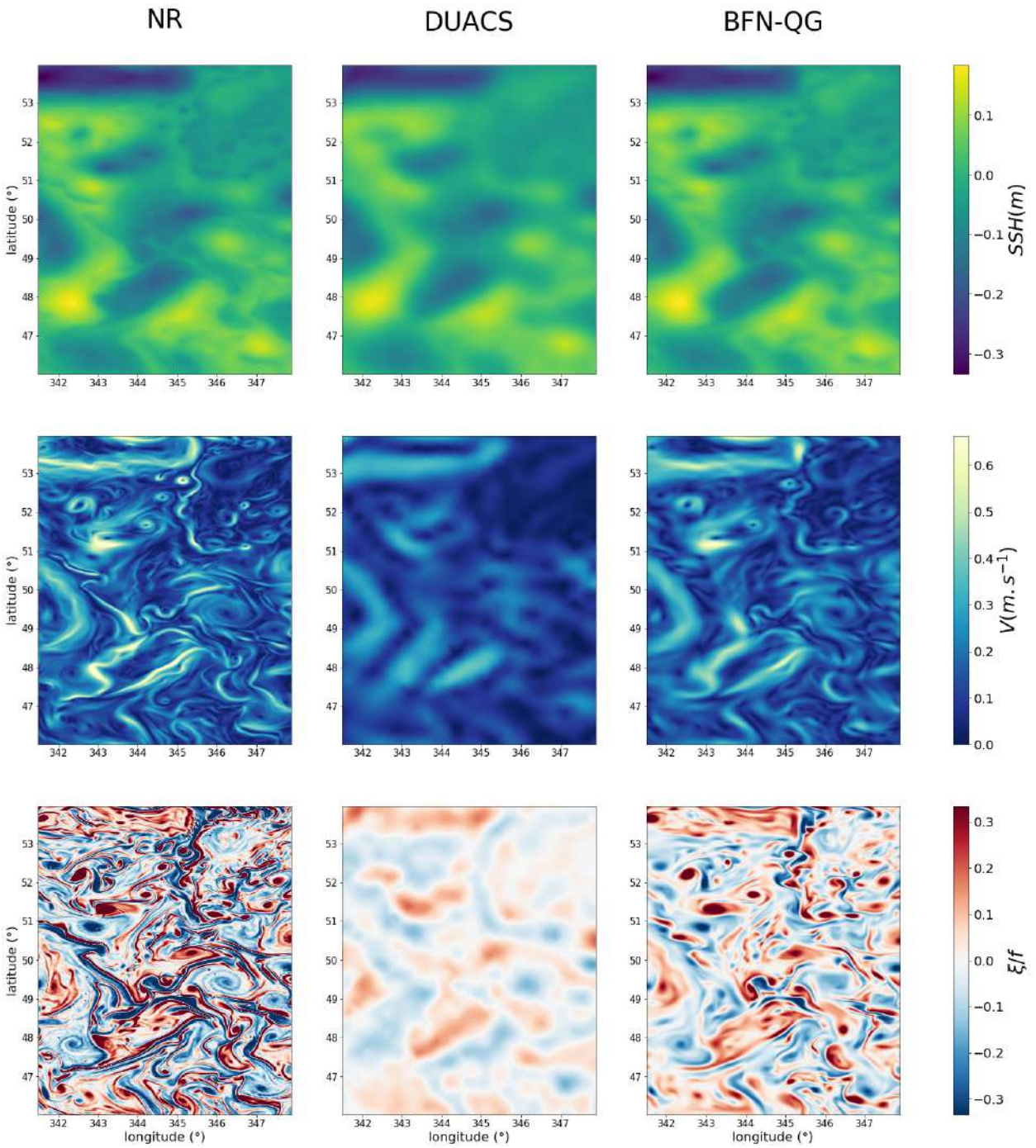

Figure 7: Snapshots of SSH (top), absolute geostrophic velocity (middle line) and normalized geostrophic relative vorticity (bottom) for the NR (left), DUACS (middle column) and BFN-QG (right) on May 26, 2013 in the OSMOSIS region. DUACS and BFN-QG are processing both nadir and SWOT data. Velocity and relative vorticity maps are computed on the native grids, i.e. before the interpolation to the (1/60° x 1/60°) grid of the NR.

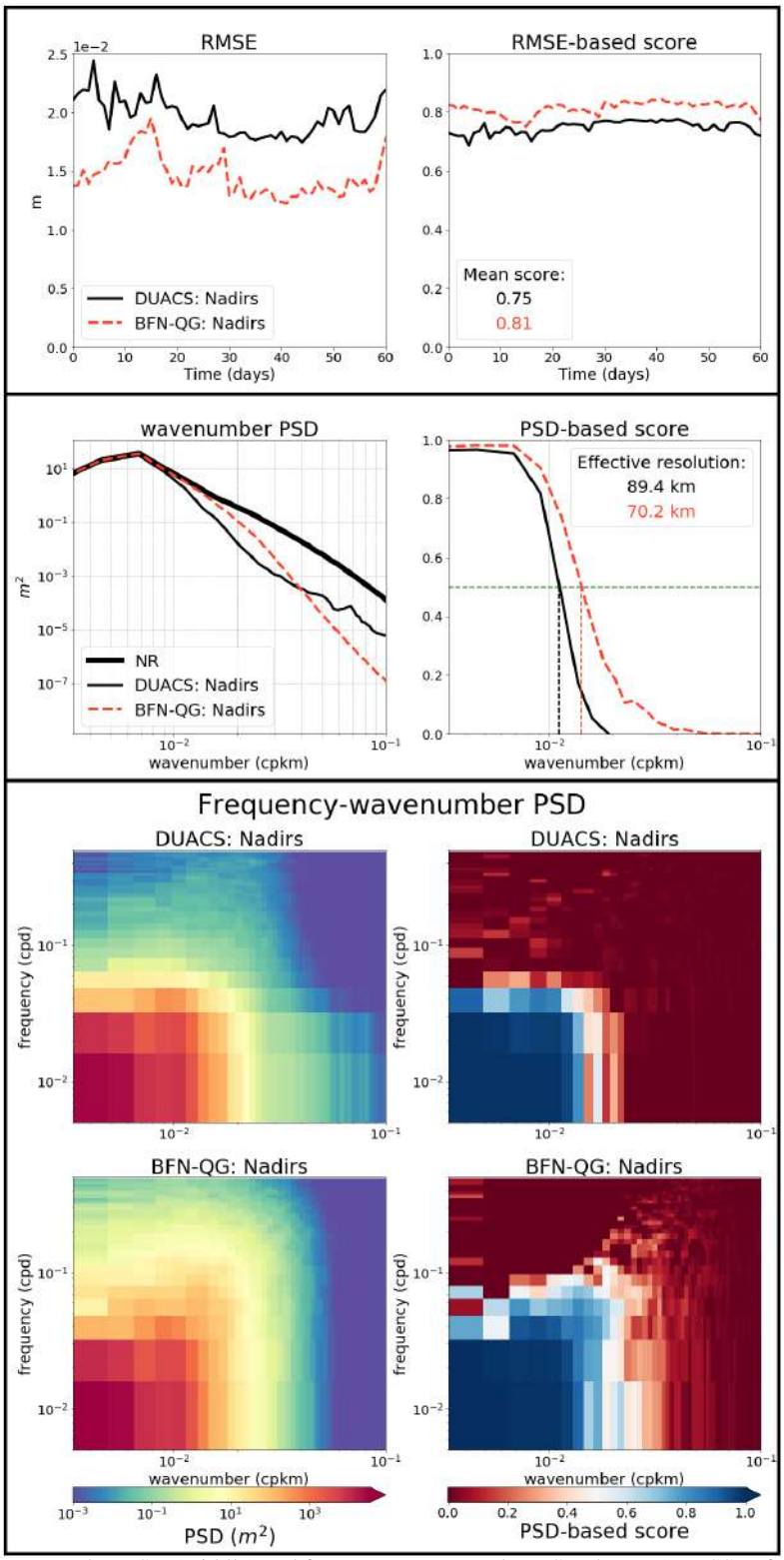

Figure 8: RMSE (top), wavenumber PSD (middle) and frequency-wavenumber PSD (bottom) on SSH, for DUACS and BFN-QG processing a constellation of 4 nadir altimeters in the OSMOSIS region during the 2 months period.

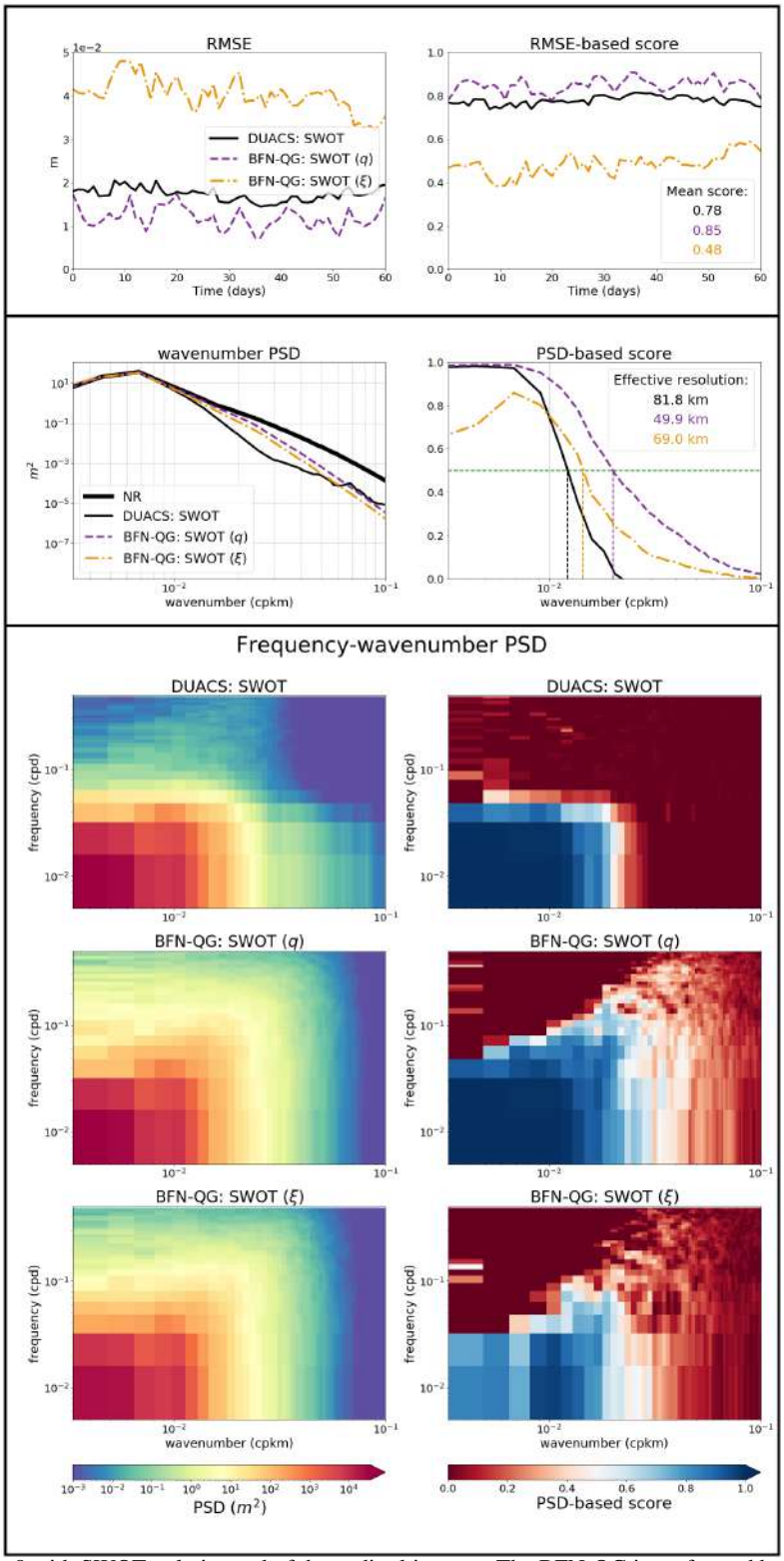

Figure 9: Same as Figure 8 with SWOT only instead of the nadir altimeters. The BFN-QG is performed by nudging SWOT data on PV (SWOT (q), purple dash line) or on relative vorticity (SWOT (ξ), orange dash line)

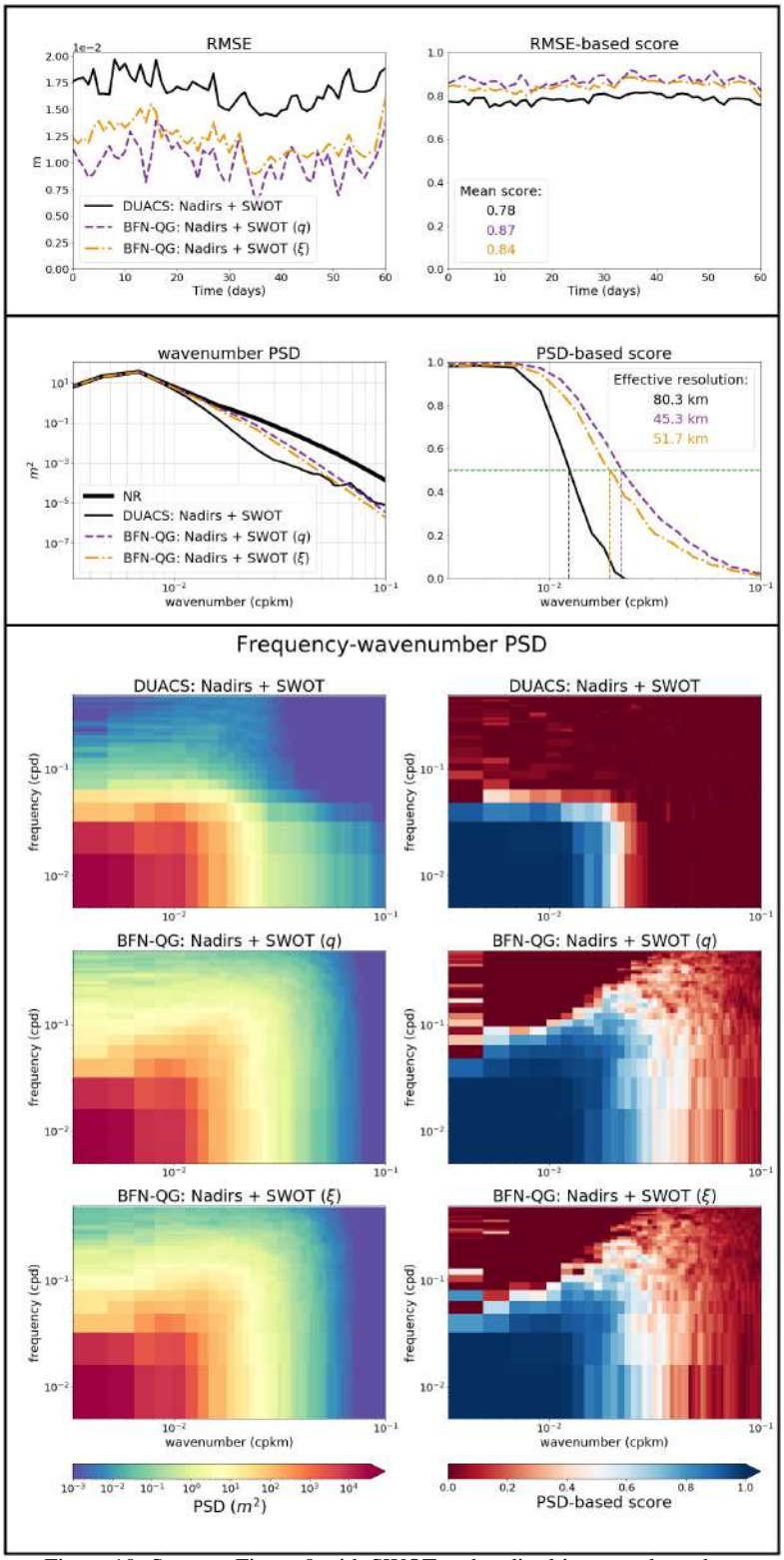

Figure 10: Same as Figure 9 with SWOT and nadir altimeters altogether.

References

Ajayi, Adekunle et al. (2020). "Spatial and Temporal Variability of the North Atlantic Eddy Field From Two Kilometric-Resolution Ocean Models". In: *Journal of Geophysical Research: Oceans* 125.5. _eprint: https://agupubs.onlinelibrary.wiley.com/doi/pdf/10.1029/2019JC015827, e2019JC015827. ISSN: 2169-9291. DOI: 10.1029/2019JC015827. URL: https://agupubs.onlinelibrary.wiley.com/doi/abs/10.1029/2019JC015827 (visited on 06/15/2020).

Chelton, Dudley B. et al. (1998). "Geographical Variability of the First Baroclinic Rossby Radius of Deformation". In: *J. Phys. Oceanogr.* 28.3. Publisher: American Meteorological Society, pp. 433–460. ISSN: 0022-3670. DOI: 10.1175/1520-0485(1998)028<0433:GVOTFB>2.0.CO;2. URL: https://journals.ametsoc.org/doi/full/10.1175/1520-0485%281998%29028%3C0433%3AGVOTFB%3E2.0.CO%3B2 (visited on 04/20/2020).

Uchida, T., R. Abernathey, and S. Smith (2017). "Seasonality of eddy kinetic energy in an eddy permitting global climate model". In: *Ocean Modelling* 118, pp. 41–58. DOI: 10.1016/j.ocemod.2017.08.006. URL: https://doi.org/10.1016/j.ocemod.2017.08.006.